J. Petit and A. Zeghloul**

On the Effect of Environment on Short Crack Growth Behaviour and Threshold

REFERENCE Petit, J. and Zeghloul, A., **On the Effect of Environment on Short Crack Growth Behaviour and Threshold**, *The Behaviour of Short Fatigue Cracks*, EGF Pub. 1 (Edited by K. J. Miller and E. R. de los Rios) 1986, Mechanical Engineering Publications, London, pp. 163–177.

ABSTRACT The growth in fatigue of physically short bidimensional cracks has been studied in air and in vacuum on the 7075 T651 high strength aluminium alloy in the low growth rate range and near threshold conditions. On the basis of crack closure measurements, and taking into account a large environmental influence, a rationalization of short and long cracks is proposed in terms of the effective stress intensity factor.

Introduction

Very few studies have been carried out on the influence of environment on the fatigue crack growth behaviour of short cracks apart from research specifically related to so called corrosive environments (**1**)(**2**). Recently Gerdes *et al.* (**3**) have shown the existence of initial propagation rates higher in air than in vacuum after initiation of short cracks in a Ti–8.6 Al alloy. Zeghloul and Petit (**4**) have shown that initial growth of short bidimensional cracks in 7075 T7351 Al alloy occurs at a very much lower stress intensity range (ΔK) level in an active environment of nitrogen containing traces of water vapour than in vacuum. Further, as inferred from long crack closure measurements (**5**), these authors have suggested that, for both environmental conditions, the crack growth rate of short bidimensional cracks could be rationalized in terms of the effective stress intensity factor range (Fig. 1(a) and (b)) which is in accordance with the observations of Breat and Pineau (**6**), and Tanaka and Nakai (**7**) working on steels.

However Lankford (**8**) has suggested the absence of any significant environmental influence on the growth of surface cracks in a 7075 T651 alloy on the basis of the observation of an overlapping of microcrack data in air and in purified nitrogen. But a comparative study of the long fatigue crack behaviour of several aluminium alloys in vacuum, ambient air and purified nitrogen (3 ppm H_2O and 1 ppm O_2) has clearly shown that the crack growth data near threshold in nitrogen is environmentally controlled with a threshold ΔK range lower than the one in vacuum and equal to or lower than the one determined in ambient air (**5**)(**9**) (Fig. 2).

To get a better understanding of the environmental influence on short crack

* Laboratoire de Mécanique et Physique des Matériaux-U.A. CNRS 863, 86034 Poitiers Cedex, France.

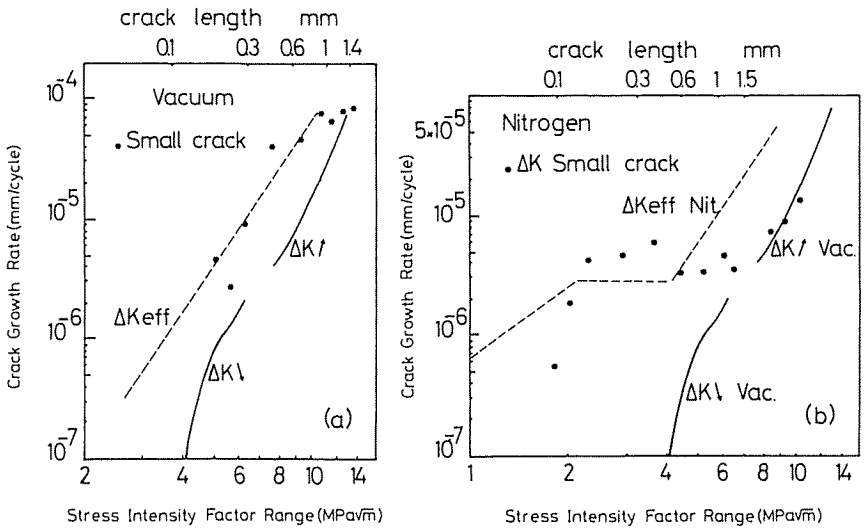

Fig 1 Crack growth rate versus ΔK for small cracks compared with long crack behaviour in terms of ΔK and ΔK_{eff}.
(a) 7075 T7351 in vacuum
(b) 7075 T7351 in vacuum and nitrogen (3 ppm H_2O)

behaviour, a study has been undertaken on the propagation of short bidimensional cracks. The present results obtained on the 7075 T651 alloy are discussed on the basis of crack closure measurements performed during tests conducted in ambient air, vacuum, and purified nitrogen.

Experimental conditions

The composition (% wt) of the 7075 T651 alloy studied was 6.0 Zn, 2.44 Mg, 1.52 Cu, 0.20 Cr, 0.16 Fe, 0.07 Si, 0.04 Mn, 0.04 Ti, Al (balance). Mechanical properties for this alloy are: yield stress 527 MPa, UTS 590 MPa, and elongation 11 per cent. The average grain size of the pancake structure is 40 × 150 × 600 μm. The microstructure of the peak aged condition is characterized by the presence of G.P. zones (about 10 Å in diameter), coherent dispersoïd plates (about 15 × 50 Å) and intermetallic constituent particles (~1 μm).

The specimens used were of 10 mm thick CT 75 type, machined in the LT direction. A long crack was first obtained at $a/W = 0.6$ by cycling at decreasing load amplitude down to threshold ($R = 0.1$, test frequency 35 Hz, in ambient air) so as to get a very small plastic zone at the crack tip. Then the plastic wake was removed by spark erosion all along the cracked surfaces so as to leave a short through-thickness crack of a length of about 0.1 mm. This technique was first proposed by Breat *et al.* (**9**) and McEvily *et al.* (**10**).

Tests were conducted in a chamber mounted on an electrohydraulic machine;

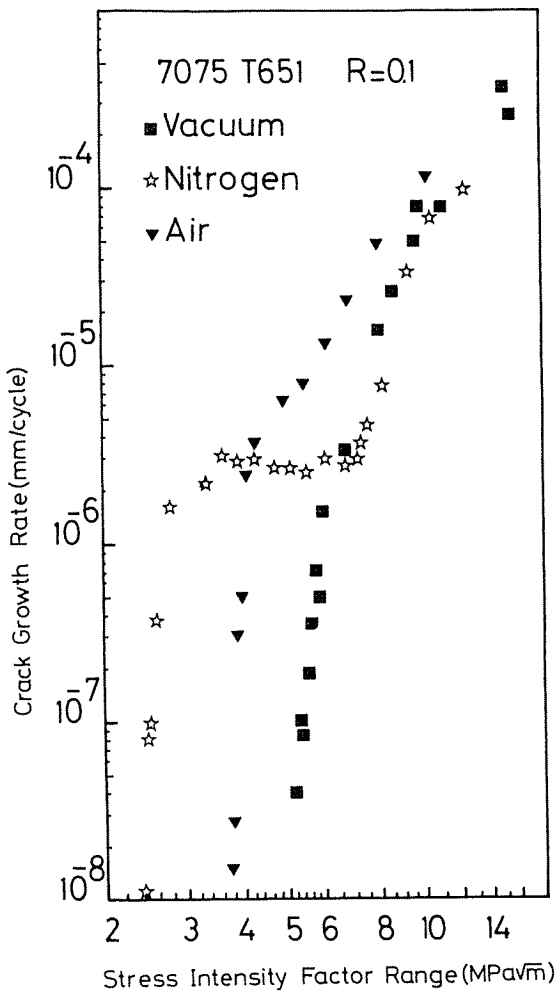

Fig 2 Crack growth rate versus ΔK for long cracks in the 7075 T651 alloy in air, vacuum, and nitrogen (3 ppm H_2O)

the environmental conditions were ambient air (~50 per cent RH) and vacuum ($<5 \cdot 10^{-4}$ Pa). A tension-tension sine wave was applied at 35 Hz with a load ratio of 0.1. Crack advance was optically monitored and crack closure was detected by means of a differential compliance technique with a gauge mounted across the notch mouth to measure the notch mouth opening δ with respect to the load P at a frequency of 0.2 Hz. Small variations of compliance were amplified using an improved differential technique (**9**)(**11**), giving $\delta' = G(\delta - \alpha_0 P)$ where G is an electronic amplification factor and α_0 the compliance of the

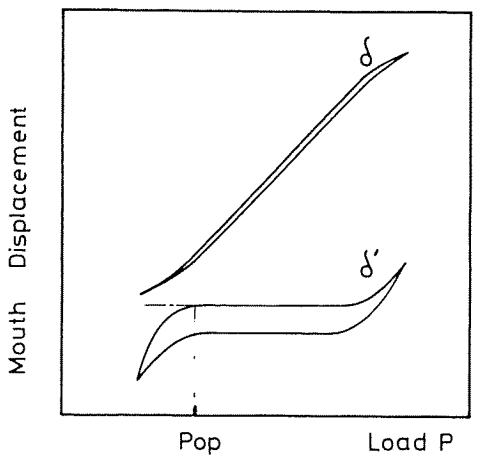

Fig 3 Determination of the load P_o corresponding to crack opening from δ vs P and differential δ' vs P diagrams

specimen with a crack fully open. From the δ' versus P diagrams the opening load P_o is defined as seen in Fig. 3.

Experimental results

Crack closure measurements were performed at different steps during machining of the crack wake (Fig. 4). The trend in the crack opening stress intensity factor K_{op} (corresponding to P_o) versus the remaining crack length Δa indicates a progressive decrease in K_{op} for values of Δa lower than 2 mm; closure becomes undetectable for a crack length of about 100 μm which is the length of the remaining short through-thickness crack. Such a length corresponds also to the limit of resolution of the compliance technique used for the detection of closure (**12**).

Further crack growth presented in Fig. 5 was performed in ambient air at decreasing load steps; the threshold level here obtained is significantly lower than the one previously determined for a long crack. Subsequent crack growth at increasing ΔK shows a progressive change in the short crack behaviour which reaches the long crack behaviour at a length about 2 mm.

The same test performed in vacuum (after machining of the wake of the crack grown in air) shows that initial growth occurs (Fig. 6) at a higher ΔK level than in air (Fig. 5). Crack arrest was obtained at the first decreasing load step (~1 million cycles) at a ΔK range of 3.6 MPa $\sqrt{m}$ instead of 5 MPa $\sqrt{m}$ for the long crack test. Further crack growth was performed under increasing ΔK conditions and, as in air, a progressive shift is observed leading to a behaviour similar to that observed for long cracks for a crack length of about 1 mm, which is shorter than the corresponding crack length in air.

The fluctuations observed in the short crack data can be related to the

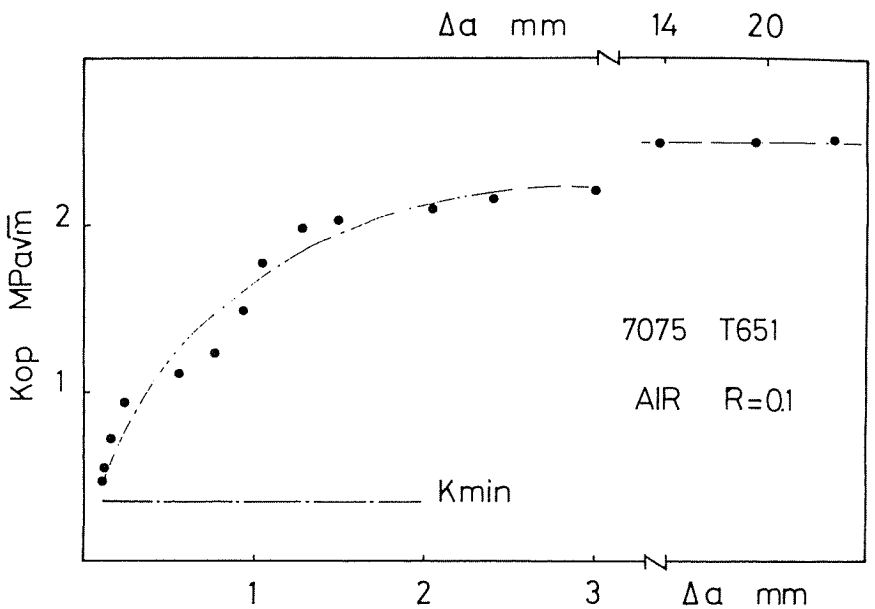

Fig 4 Variation of the opening stress intensity factor K_{op} as a function of the remaining crack length Δa after machining of the crack wake on the 7075 T651 alloy

changes detected in the crack growth direction; the crack profile (Fig. 7) observed on one of the faces of the specimen exhibits evidence of crack deflection and crack branching at the high angle grain boundaries all along the crack path in vacuum starting at the level of the two microhardness imprints. So, the above fluctuations can be related to a microstructural influence on crack growth.

Crack closure measurements (Fig. 8) show a progressive increase in K_{op} during the short crack growth. The K_{op} development with respect to short crack length in air is similar to the one obtained from machining the plastic wake (the dash-dotted curve in Fig. 8 is from Fig. 4). Such a result indicates that the experimental procedure has little influence on closure measurements.

In vacuum, K_{op} increases also with respect to the crack length but more rapidly than in air. This result is consistent with the observation of a shorter 'short crack effect' in vacuum.

Figure 9 compares the short crack data expressed in terms of the effective stress intensity range ΔK_{eff} ($= K_{max} - K_{op}$) with results obtained for long cracks. A good correlation is observed in vacuum and, consequently, short and long crack behaviour appears to be rationalized in term of ΔK_{eff}. Compared to vacuum, a poorer agreement is observed in air between short and long cracks growth rates; however, the general trend is consistent with the observation made in vacuum.

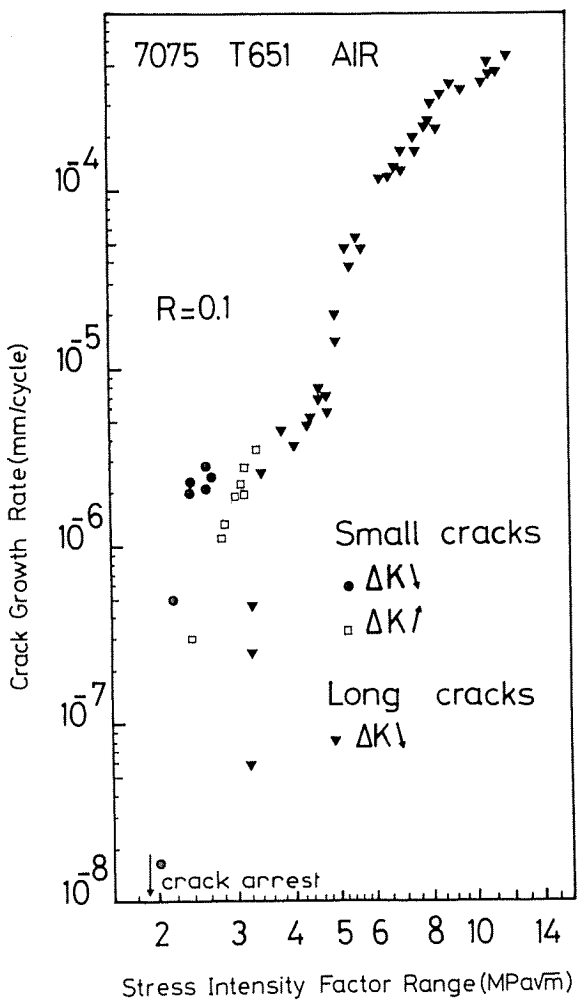

Fig 5 Crack growth rate versus ΔK in air for small cracks compared with long crack behaviour in the 7075 T651 alloy

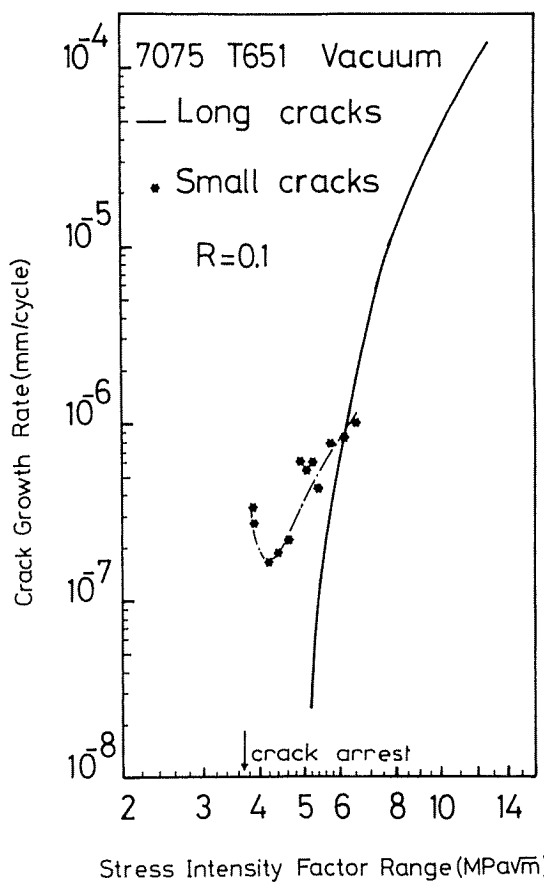

Fig 6 Crack growth rate versus ΔK in vacuum for small cracks compared with long crack behaviour in the 7075 T651 alloy

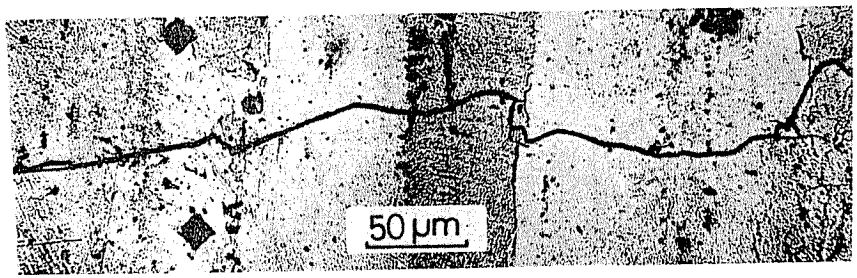

Fig 7 Micrographic observation of the crack profile in the 7075 T651 alloy tested in vacuum. The initial crack length corresponds to the microhardness indents (~ 0.17 mm)

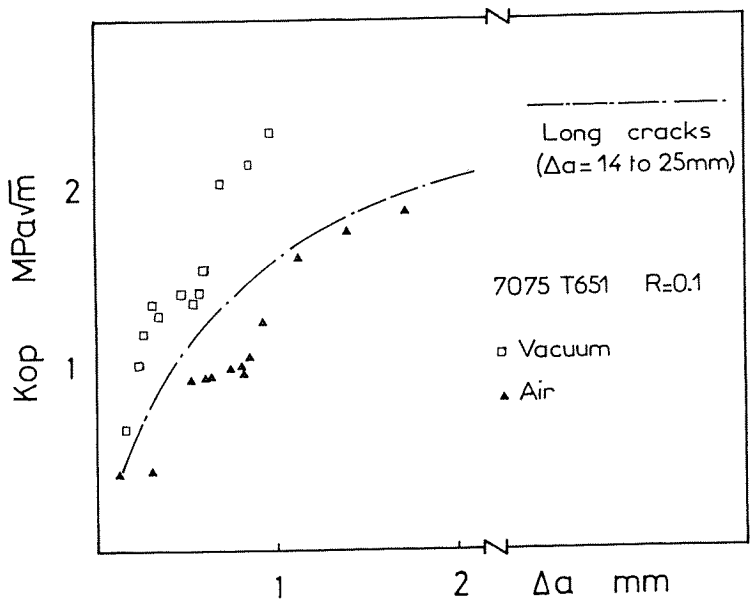

Fig 8 Variation of the opening stress intensity factor K_{op} in air and vacuum as a function of Δa the short crack length; 7075 T651 alloy

The results are consistent with dominant crack closure effects controlling the crack growth behaviour of bidimensional through-thickness short cracks and confirm observations made by different authors (**6**)(**10**)(**13**)(**14**). In addition, these results show a substantial influence of environment on crack growth rates and threshold ranges. The following discussion will be essentially focussed on the environmental influence.

Discussion

Figure 10 compares the long crack growth data expressed in terms of ΔK_{eff}

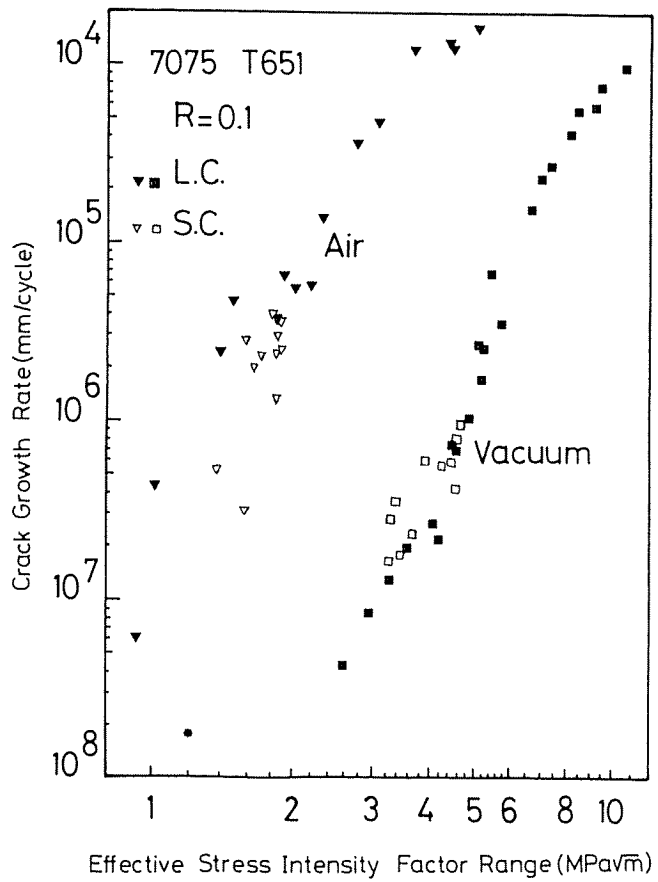

Fig 9 Crack growth rate versus ΔK_{eff} for small and long cracks in air and vacuum; 7075 T651 alloy

obtained on the 7075 T651 alloy tested at $R = 0.1$ and 35 Hz in vacuum, ambient air and purified nitrogen. This figure is quite complex and can be explained only on the basis of previously obtained results on different aluminium alloys and especially the 7075 alloy in the underaged (T351) and overaged conditions (T7351) (**5**).

In the absence of any environmental effect, in vacuum, the crack propagation mechanism is governed only by microstructural factors whose action in turn is governed by the loading conditions. The crack propagation is intergranular controlled by slip in one or many active planes. In the crack growth range where the Paris law is valid, i.e., in stage II (Fig. 10), the crack tip loading conditions permit at least two slip systems to be active (**15**) which in turn leads to a plane crack growth path affected only by the presence of large inter-metallic precipi-

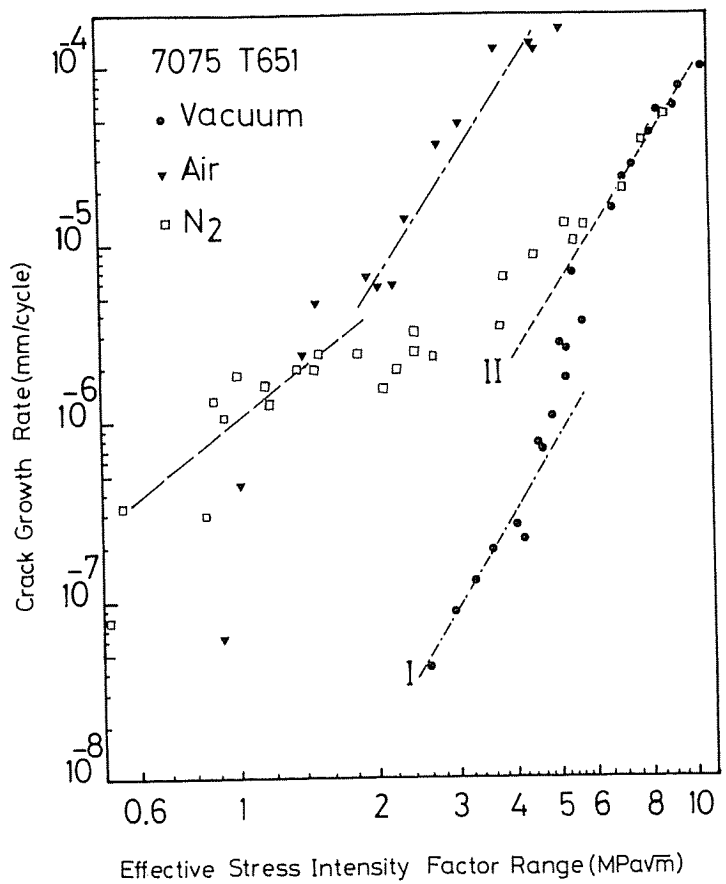

Fig 10 Crack growth rate versus ΔK_{eff} for long cracks on the 7075 T651 alloy in air, vacuum, and nitrogen (3 ppm H_2O)

tates. In the range which represents the transition from stage II to stage I, ($da/dN \sim 3 \cdot 10^{-6}$ mm/cycle), a crystallographic crack propagation mode is observed (Regime I in Fig. 10) corresponding to planar slip and where slip is localized to a single system. A similar process was analysed in the case of a Ni-based super-alloy with γ' hardening precipitates (**16**) and the above mentioned transition was attributed to the existence of deformation levels lower than that required for the saturation of slip bands near the crack tip. A similar mechanism may be present in the 7075-T651 alloy with coherent GP zones and dispersoid plates (15 × 50 Å), leading to low crack propagation rates and high thresholds ($\Delta K_{th} = 5.5$ MPa$\sqrt{m}$ and $\Delta K_{eff \cdot th} \sim 2.5$ MPa$\sqrt{m}$).

The crack propagation in vacuum can be represented by a law derived from Weertman's model (**17**)

$$\frac{da}{dN} = \frac{A(\Delta K_{eff})^4}{\mu \sigma^2 \gamma} \quad (1)$$

where A is a dimensionless constant, σ flow stress, μ shear modulus, and γ the energy required to create a unit free surface.

The environmental effect consists of two distinct processes which are water adsorption and oxidation. The adsorption of water vapour molecules on the freshly created surfaces at the crack tip leads to reduction in the atomic bond strength in the case of tensile and shear type deformation (Rehbinder effect (**18**)); this phenomenon results in a decrease of fatigue strength and consequently to a reduction in the value of energy, γ. When the time required for the creation of a single layer of adsorbed molecules at the crack tip is attained in each cycle, the adsorption effect is saturated and an acceleration of crack growth is observed without any change in crack propagation mechanism, which remains similar to that in vacuum, only the value of γ is diminished. Typically, this effect is observed in the 7075-T651 alloy in air at medium growth rates.

In the case where gas transport at the crack tip does not result in the formation of an adsorbed layer (even partial), no environmental effect is observed. Such a situation exists in high purity N_2 in the mid rate range where the crack growth behaviour in this environment is similar to the one in vacuum. When the conditions existing at the crack tip permit the creation of a partial adsorbed layer, local crack growth acceleration is observed as in the transition range in the N_2 environment. In this range the crack growth curve in N_2 shifts from a behaviour similar to that in vacuum (negligible adsorption effect) to a behaviour similar to that in air (saturated adsorbed layer): the degree of gas coverage of freshly created surfaces varies from zero as in vacuum to unity as in air during this transition which takes place in the range $2 \cdot 10^{-6} < da/dN < 10^{-5}$ mm/cycle.

The conditions determining the access of the active species (H_2O molecules in this case) depends upon many factors, such as the geometry of the crack, the test frequency, the R ratio, the trapping of water molecules by oxide deposits, and the partial pressures of water vapour molecules.

The chemisorption phenomenon describes the formation of hydrogen by the dissociation of the adsorbed water molecules (**19**). In such a case a hydrogen embrittlement mechanism can be brought into action (**20**)–(**22**). The concentration of hydrogen in the process zone can be sufficient only if the adsorption effect is saturated. The attainment of this critical concentration is time dependent (time for hydrogen diffusion by dislocation dragging and time for water vapour transport at the crack tip) and can be favoured by the localized deformation in a single slip system. In the 7075-T651 alloy such a condition seems to prevail only for crack growth rates of the order of $5 \cdot 10^{-6}$ mm/cycle, particularly in N_2.

This hydrogen assisted crack propagation can be associated with a mechanism of crack propagation controlled by the crack tip opening displacement range ΔCTOD (**23**) described by a relation of the type

$$\frac{da}{dN} = B(\Delta K_{eff})^2/\mu\sigma^2 \qquad (2)$$

The flow stress in this case is characteristic of the embrittled material at the crack tip. Under such conditions the crack growth resistance is much smaller than that in vacuum, resulting in a very low threshold (ΔK_{th} = 2.4 MPa$\sqrt{m}$, $\Delta K_{eff \cdot th} \sim 0.5$ MPa$\sqrt{m}$ in nitrogen).

In air a different situation exists; as in the presence of O_2 molecules at a high partial pressure and at low R values, the crack surfaces are oxidized by a fretting action (**24**)–(**26**). In the 7075-T651 alloy the oxide thickness is smaller than the ΔCTOD value (**26**) which precludes the 'wedging effect' observed in steels (**24**). At the same time, the presence of this oxidized layer can constitute a water-vapour trap, thus rendering difficult the access of the active species at the crack tip. This effect can explain the existence of a higher threshold in air than in N_2 at R = 0.1. The fact that the threshold values at an R value of 0.5 is the same in similar aluminium alloys adds weight to this hypothesis (**5**).

The short crack behaviour presented in Figs 5, 6, and 9 can be analysed on the basis of these considerations. In vacuum, the crack growth mechanism appears to be the same as the one described for a long crack and is rationalized in terms of ΔK_{eff}. The crack profile presented in Fig. 7 is also consistent with a single slip mechanism in the explored rate range. The fundamental difference between short and long crack data consists in the influence of crack length on closure. Closure for long cracks on this alloy tested in vacuum is essentially related to the very high roughness of the cracked surfaces due to the crystallographic mode of failure. The amount of closure is consequently directly related to the crack wake and the loading history. So qualitatively, a large influence of short crack length must be expected in this alloy.

In air, there exists a more complex situation. Near the threshold crack growth has been shown to be strongly dependent upon the factors which determined the conditions of access of active species (i.e., water vapour) to the crack tip, as indicated above. The respective effects of these various factors which influence $\Delta K_{eff \cdot th}$ and the near threshold crack growth are very difficult to analyse. The poor agreement between short and long crack data in Fig. 9 could be related to some difference in the effects of these factors. In addition, for closure measurements, in the low ΔK range, the experimental scatter in air is large (about 30 per cent at K_{op}). Further experiments are necessary to clarify such behaviour. However, the general trend is consistent with the behaviour of a long crack with the observation of an effective threshold higher than the one in nitrogen, which suggests an oxidation effect.

As suggested by Beevers (**27**) the threshold range can be analysed in two components

$$\Delta K_{th} = \Delta K_i + \Delta K_c \qquad (3)$$

where $\Delta K_i = \Delta K_{eff \cdot th}$ is the intrinsic component and ΔK_c the closure contribution.

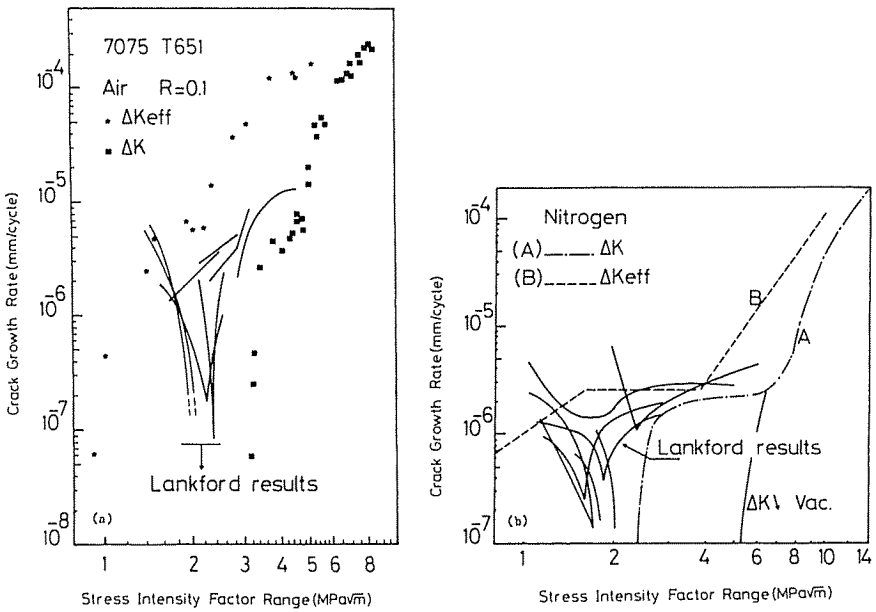

Fig 11 Small cracks compared to long crack behaviour for the 7075 T651 alloy.
(a) in air
(b) in nitrogen (2 to 3 ppm H_2O) (8)

On the basis of the present results and the previous observations on long cracks, this analysis of ΔK_{th} could be extended to a short bidimensional crack with ΔK_c again being dependent on the same factors as a long crack (plasticity, roughness, oxidation, microstructure, slip mechanisms) but now depending also on the crack length. Then the lower bound for short crack thresholds should be ΔK_i. That would mean that no crack growth can be observed in any case for ΔK lower than ΔK_i so long as the effective value of ΔK can be accurately determined.

Another limitation of these concepts is the extent and the shape of the crack considered. The present study was carried out on short through-thickness cracks; for example, Lankford studied semi-elliptic surface cracks, which were typically three-dimensional cracks and were smaller by an order of magnitude. As discussed by different authors the application of LEFM to calculate ΔK in such cases appears to be questionable (**28**). However, it is of some interest to compare the long crack data expressed in terms of ΔK and ΔK_{eff} to the Lankford data obtained on the same alloy in air and in purified nitrogen (2 ppm H_2O) (Fig. 11). It can be seen that, globally, the short crack data fall between the da/dN vs ΔK and da/dN vs ΔK_{eff} curves. This consideration appears to be consistent with a dominant role of closure for this kind of crack. In addition the comparison of the data in air (Fig. 11(a)) and in nitrogen (Fig. 11(b)) illustrates

the existence of a large environmental effect in both environmental conditions and explains the absence of environmental influence observed by this author, except for a slightly higher influence in nitrogen, with the crack growing at lower ΔK values than in air.

Conclusions

(1) The growth of physically short bidimensional cracks can be rationalized with that for long cracks in terms of ΔK_{eff}

(2) In the low growth rate range and near the threshold condition, two typical da/dN vs ΔK_{eff} relations can be defined corresponding to pure active or pure inert environments which can be simulated, respectively, at near threshold conditions by a purified inert gas containing water vapour traces (about a few ppm) and high vacuum.

(3) Two characteristic effective stress intensity ranges at the threshold correspond to these two critical environmental conditions.

(4) In ambient air, and specifically at low R ratio, an intermediate growth behaviour is observed due to a more or less pronounced inhibition of the water vapour effect by such closure induced phenomena as crack surface oxidation.

(5) Considering that the threshold range can be analysed in two components, the lower threshold ranges generally observed for short cracks correspond to a decrease in the closure component with crack length, while the intrinsic component is sensitive only to environment.

References

(1) GANGLOFF, R. P. (1985) Crack size effects on the chemical driving force for aqueous corrosion fatigue, *Met. Trans*, **16A**, 963.

(2) SURESH, S. and RITCHIE, R. O. (1984) Near threshold fatigue crack propagation: a perspective on the role of crack closure, *Fatigue crack growth threshold concepts* (Edited by Davidson, D. and Suresh, S.), (Metallurgical Society of AIME), pp. 227–261.

(3) GERDES, C., GYSLER, A., and LUTJERING, G. (1984) Propagation of small surface cracks in Ti-alloys, *Fatigue crack growth threshold concepts* (Edited by Davidson, D. and Suresh, S.), (Metallurgical Society of AIME), pp. 465–478.

(4) ZEGHLOUL, A. and PETIT, J. (1985) Environmental sensitivity of small crack growth in 7075 aluminium alloy, *Fatigue Fracture Engng Mater. Structures*, **8**, 341–348.

(5) PETIT, J. (1984) Some aspects of near-threshold crack growth: microstructural and environmental effects, *Fatigue crack growth threshold concepts* (Edited by Davidson, D. and Suresh, S.), (Metallurgical Society of AIME), pp. 3–24.

(6) BREAT, J. L., MUDRY, F., and PINEAU, A. (1983) Short crack propagation and closure effects in A508 steel, *Fatigue Engng Mater. Structures*, **6**, 349–358.

(7) TANAKA, K. and NAKAI, Y. (1983) Propagation and non-propagation of short fatigue cracks at a sharp notch, *Fatigue Engng Mater. Structures*, **6**, 315–327.

(8) LANKFORD, J. (1983) The effect of environment on the growth of small fatigue cracks, *Fatigue Engng Mater. Structures*, **6**, 15–31.

(9) PETIT, J. and ZEGHLOUL, A. (1982) Gaseous environmental effect on threshold level in high strength aluminium alloys, *Fatigue thresholds* (Edited by Bäcklund, J., Blom, A. F., and Beevers, C. J.), (EMAS, Warley, UK), pp. 563–579.

(10) MINNAKAWA, K., NEWMAN, J. C., and McEVILY, A. J. (1983) A critical study of the crack closure on near-threshold fatigue crack growth, *Fatigue Engng Mater. Structures*, **6**, 359–365.

(11) OHTA, A. and SASAKI (1975) a method for determining the stress intensity threshold level for fatigue crack propagation, *Int. J. Fracture*, **17**, 1040–1050.

(12) JAMES, M. N. and KNOTT, J. F. (1985) Critical aspects of the characterization of crack tip closure by compliance techniques, *Mat. Sci. Engng*, **72**, L1–L4.

(13) JAMES, M. R. and MORRIS, W. L. (1983) Effect of fracture surface roughness on growth of short fatigue cracks. *Met. Trans*, **14A**, 153–155.

(14) McCARVER, J. F. and RITCHIE, R. O. (1982) Fatigue crack propagation thresholds for long and short cracks in 95 nickel-base superalloy, *Mat. Sci. Engng*, **55**, 63–67.

(15) DAVIDSON, D. L. and LANKFORD, J. (1984) Fatigue crack growth mechanisms for Ti-6Al-4V (RA) in vacuum and humid air, *Met. Trans*, **15A**, 1931–1940.

(16) VINCENT, J. N. (1986) *Comportement en fatigue d'un alliage à base de nickel à gros grains: mécanismes de déformation et d'endommagement liés à cristallographie*, Doc. ès. Sci. thesis, Paris XI.

(17) WEERTMAN, J. (1973) Theory of fatigue crack growth based on a BCS theory work hardening, *Int. J. fracture Mech.*, **9**, 125–137.

(18) WESTWOOD, A. R. C. and AHEARN, J. S. (1984) Adsorption sensitive flow and fracture of solids, *Physical chemistry of the solid state: applications to metals and compounds* (Edited by Lacombe, J.), (Elsevier, Amsterdam), vol. 32, pp. 65–85.

(19) BOWLES, C. Q. (1978) The role of environment frequency and wave shape during fatigue crack growth in aluminium alloys, Report L.R. 270 Delft University of Technology, The Netherlands.

(20) CHAKRAPANI, D. G. and PUSH, E. N. (1976) Hydrogen embrittlement in a Mg–Al alloy, *Met. Trans*, **7A**, 173–178.

(21) JACKO, R. J. and DUQUETTE, D. J. (1977) Hydrogen embrittlement of a cyclically deformed high strength Al alloy, *Met. Trans*, **8A**, 1821–1827.

(22) ALBRECHT, J., McTIERNAN, B. J., BERNSTEIN, I. M., and THOMPSON, A. W. (1977) Hydrogen embrittlement in a high-strength aluminium alloy, *Scripta Met.*, **11**, 893–897.

(23) LANKFORD, J. and DAVIDSON, D. L. (1983) Fatigue crack micromechanisms in ingot and powder metallurgy 7XXX aluminium alloys in air and vacuum, *Acta. Met.*, **31**, 1273–1284.

(24) SURESH, S., ZAMISKI, G. F., and RITCHIE, R. O. (1981) Oxide induced crack closure: an explanation for near-threshold corrosion fatigue crack growth behavior, *Met. Trans*, **12A**, 1435–1443.

(25) VASUDEVAN, A. K. and SURESH, S. (1982) Influence of corrosion deposits on near-threshold fatigue crack growth behavior in 2XXX and 7XXX series aluminium alloys, *Met. Trans*, **13A**, 2271–2280.

(26) RENAUD, P., VIOLAN, P., PETIT, J., and FERTON, D. (1982) Microstructural influence on fatigue crack growth near threshold in 7075 Al alloy, *Scripta Met.*, **16**, 1311–1316.

(27) WALKER, N. and BEEVERS, C. J. (1979) A fatigue crack closure mechanism in titanium. *Fatigue Engng Mater. Structures*, **1**, 135–148.

(28) MILLER, K. J. (1982) The short crack problem, *Fatigue Engng Mater. Structures*, **5**, 223–232.